ORIGINAL ARTICLE

A C G publications

Rec. Nat. Prod. X:X (202X) XX-XX

records of natural products

Butanedioic Acid Benzyl Ester Glycosides from *Pleione bulbocodioides* (Franch.) Rolfe: Promising Fungicide Against *Phoma herbarum*

Shilin Liu [1#], Jiarui Fu [1#], Yuping Fu [1], Yuanan Chen [1], Lijun Zhen [2], Huiyou Xu [1] and Lin Ni [1*]

[1] *College of Plant Protection, Fujian Agriculture and Forestry University, Fuzhou 350002, People's Republic of China*

[2]*Department of Pharmacy, Fujian Medical University Union Hospital, Fuzhou 350002, People's Republic of China*

(Received April 28, 2024; Revised June 04, 2024; Accepted June 09, 2024)

Abstract: The bioactive compounds of the pseudobulbs of *Pleione bulbocodioides* were isolated, purified, and identified using modern spectroscopic techniques, which identified seven butanedioic acid compounds. Compounds **1-3**, **5**, and **6** were isolated for the first time from *Pleione bulbocodioides*. The antifungal activity of the seven compounds was evaluated through cytotoxic activity assays, revealing that compound **4**, militarine, exhibited moderate inhibitory activity against *Phoma herbarum*, with an effective concentration (EC_{50}) of 68.575 μg/mL. We get further deep insight into the antifungal mechanism of militarine against *Phoma herbarum* through electron microscopy, transcriptomics, and changes in physiological and biochemical indicators. Transcriptomic sequencing revealed 216 significantly upregulated differentially expressed genes and 277 significantly downregulated differentially expressed genes. Gene ontology (GO) and Kyoto Encyclopedia of Genes and Genomes (KEGG) enrichment analysis showed that differentially expressed genes were involved in pathways related to secondary metabolism, biosynthesis, membrane components, nitrogen metabolism, and ATP-binding cassette (ABC) transporter, suggesting that militarine may inhibit the normal growth of hyphae through these pathways.

Keywords: *Pleione bulbocodioides*; *Phoma herbarum*; chemical composition; antifungal mechanism.

1. Introduction

Phoma herbarum, belonging to the subphylum *Pezizomycotina*, class *Dothideomycetes*, order *Pleosporales*, family *Phaeosphaeriaceae*, genus *Phoma spp.* [1]. This genus has promising cellulase activity, most species within this genus are plant pathogens, primarily affecting stems, branches, leaves, and fruits, causing stem rot, twig blight, and necrosis of leaves and fruits in crops, with lesions showing indistinct margins [2]. For instance, *Phoma lingam* causes blackleg disease in cruciferous plants [3];

*Corresponding author: E-mail: nilin_fjau@126.com
#Shilin Liu and Jiarui Fu contribute equally to the article

The article was published by ACG Publications
http://www.acgpubs.org/journal/records-of-natural-products Month-Month 2024 EISSN:1307-6167
DOI: http://doi.org/10.25135/rnp.466.2404.3217
Available online: July 01, 2024

Phoma betae induces *Phoma* leaf spot in sugar beets [4]; *Phoma adianticola* causes brown bud disease in tea trees [5]. As a pathogen, *P. herbarum* can cause leaf spot disease in *Atractylodes lancea* [6], and buckwheat ring rot disease in *Fagopyrum esculentum* Moench [7], and it can also infect various plants such as *Commelina communis*, *Polygonatum sibiricum*, *Nymphaea alba*, and *Pennisetum* [8-11]. Currently, there are no established measures to effectively manage these diseases. The routine approach involves the use of chemical pesticides, such as thiophanate-methyl and chlorothalonil, for disease control. However, the excessive utilization of these chemical fungicides has led to environmental pollution, the development of pathogen resistance, and other adverse consequences. [12]. Consequently, it is imperative to quest for fungicides that are efficient, safe, and environmentally friendly in order to manage these diseases effectively.

Pleione bulbocodioides (Franch.) Rolfe is a species of plant belonging to the *Orchidaceae* family, within the *Pleione* genus. [13]. With its unique beauty and rarity, there are about 26 wild varieties worldwide. These plants are widely distributed, stretching from the Qinling Mountains in China to the southwest, covering the mountainous regions of central and eastern China and Taiwan. Their distribution is not limited to China, but also extends to the western region of the Himalayas, including India, Nepal, Myanmar, Laos, Thailand, and other countries. Most of these countries belong to the subtropical zone and the cooler regions of the tropics [14]. In addition to its striking ornamental value, it also has a rich medicinal value and has a long history as one of the precious medicinal materials in traditional Chinese medicine. According to the Chinese Pharmacopoeia, the *Pleione bulbocodioides* is sweet and slightly pungent, cool in nature, and has the effects of dissolving phlegm, clearing heat and detoxifying, and is used for the treatment of lymph node tuberculosis and sputum nucleus [15]. Previous reports indicate that a total of 85 chemical constituents belonging to 10 types, including phenols, benzyl compounds, and butanedioic acid derivatives, have been isolated from *Pleione* species [16-20]. Butanedioic acid benzyl ester glycosides, characterized as typical chemical constituents of *Orchidaceae*, consist of butanedioic acid as the basic nucleus, often combined with sugars to form glycosides. However, literatures regarding such compounds from *Pleione* species are relatively scarce. Our research group has been dedicated to the development and utilization of medicinal resources from *Pleione bulbocodioides*, and isolated seven butanedioic acid benzyl ester glycoside compounds. Earlier research has demonstrated that ethanol extracts derived from the pseudobulbs of *Pleione bulbocodioides* possess broad-spectrum antifungal properties against plant pathogens [21]. Initial investigations have primarily concentrated on elucidating their mechanisms of action. Building upon this foundation, this study aims to delve deeper into the butanedioic acid benzyl ester glycoside compounds present in ethanol extracts of *Pleione bulbocodioides* pseudobulbs, particularly focusing on *P. herbarum* as a representative target, to explore the antifungal activity mechanisms of active. This research endeavors to provide scientific insights for the further development and utilization of *Pleione bulbocodioides*.

2. Instruments and Materials

2.1. Instruments

Bruker Avance III 400 MHz spectrometer (Bruker, Germany), Laser confocal microscope TCS SP8 Leica, Germany, Waters W2695-QDA High Performance Liquid Chromatography-Mass Spectrometry (HPLC-MS) System (Waters Corporation), LC-20AP Preparative High Performance Liquid Chromatography System (Shimadzu), THZ-C-1 Benchtop Refrigerated Oscillator (Suzhou Peiying Laboratory Equipment Co., Ltd.), SPX-250B-Z Biochemical Incubator (Suzhou Changliu Purification Technology Co., Ltd.), SW-CJ-1C All-steel Double-Person Single-sided Horizontal Laminar Flow Clean Table (Suzhou Bolel Purification Equipment Co., Ltd.), GR85DF High Pressure Sterilizer (American Zhiwei Instrument Co., Ltd.), UVmini-1240 UV-Vis Spectrophotometer (Shimadzu), EPOCH2 Microplate Reader (BioTek Instruments, Inc.).

2.2. Materials

Silica gel (Qingdao Ocean Chemical Co., Ltd.); Sephadex LH-20 Gel (Shanghai Yuanye Biotechnology Co., Ltd); PRP-512A Resin (Beijing Jufu Resin Factory); YMC-Pack ODS-A Reversed-Phase Chromatography Column (YMC Co., Ltd., Japan); Diamonsil C18 Analytical Reversed-Phase Chromatography Column (Beijing Dimachem Technology Co., Ltd.); Organic solvents including methanol, dichloromethane, petroleum ether, and ethyl acetate (Xilong Chemical Co., Ltd.); Chromatography-grade methanol and acetonitrile purchased from Merck & Co., Inc.; Eugenol (Shandong Yijia Agricultural Chemical Co., Ltd.); Potatoes (purchased from Yonghui Supermarket); Distilled water (prepared in the laboratory); Formaldehyde Activity Test Kit, Reducing Sugar Content Test Kit, Enzyme Activity Test Kit, 4',6-Diamidino-2-phenylindole dihydrochloride (DAPI), Reactive Oxygen Species Test Kit (Beijing Solarbio Science & Technology Co., Ltd); Calcofluor White (CFW) (Shanghai Maclyn Biochemical Technology Co., Ltd.).

Pseudobulbs of *Pleione bulbocodioides* (produced in Guizhou Province, China, and the production lot number is 20200701) were purchased from Hongkang Traditional Chinese Medicine Decoction Pieces Co., Ltd in Yichun, Jiangxi Province, and identified by Associate Professor Zou Xiaoxing from the College of Forestry, Fujian Agriculture and Forestry University. The samples were preserved in the Department of Pesticides and Pharmaceutical Engineering, College of Plant Protection, Fujian Agriculture and Forestry University.

The *Phoma herbarum* was provided by the Key Laboratory of Biopesticide and Chemical Biology, Fujian Agriculture and Forestry University.

3. Experiment Methods

3.1. Extraction of Chemical Components

The pseudobulbs of *Pleione bulbocodioides* were crushed into coarse powder, with 10 kg weighed for extraction. Reflux extraction was carried out twice using 80 L of 75% methanol at 80 °C for 2 hours each time. The resulting extract was filtered through cheesecloth, and the filtrates from both extractions were pooled. This combined extract was then concentrated under reduced pressure, yielding 2.45 kg of herbal extract. The extract was dissolved in 30 L of distilled water and purified using D101 macroporous adsorption resin. Sequential elution was performed using water (45 L), followed by 10% (27 L), 30 % (27 L), 60 % (27 L), and 90 % (27 L) ethanol solutions. The eluates were collected separately, and the aqueous eluate was discarded. The remaining four eluates were concentrated under reduced pressure to yield four subfractions: DSL-1 (87.01 g), DSL-2 (308.31 g), DSL-3 (156.44 g), and DSL-4 (145.00 g).

DSL-3 underwent silica gel chromatography (75~50 μm) for purification, utilizing a dichloromethane-methanol gradient system (20:1, 10:1, 5:1, 3:1, 1:1, methanol), resulting in the isolation of seven components (DSL-3-1~7). DSL-3-4 (21.4 g) was separated using PRP512A resin and eluted sequentially with 10%, 30%, 50%, 75%, and 100% ethanol, yielding five components (DSL-3-4-1~5). DSL-3-4-1 (7.19 g) underwent further purification through medium-pressure column chromatography (16~80 μm) using a dichloromethane-methanol gradient system (7:1, 5:1, 3:1, methanol), resulting in the isolation of 11 components. Among them, DSL-3-4-1-7 was recrystallized to obtain a larger quantity of compound **4** (2.29 g). DSL-3-4-1-3 (1.19 g) was purified through preparative liquid chromatography (C18, 60% methanol, 8.0 mL·min^{-1}, 210 nm), yielding compounds **2** (107.5 mg) and **3** (72.3 mg). DSL-3-4-2 (5.78 g) underwent gel column chromatography with methanol as the eluent, resulting in the collection of fractions, which were detected by TLC and combined to obtain nine components (DSL-3-4-2-1~9). DSL-3-4-2-4 (181.8 mg) was further purified through preparative liquid chromatography (C18, 30% acetonitrile, 3.0 mL·min^{-1}, 210 nm), yielding compounds **1** (26.6 mg).

DSL-4 was mixed with diatomite in a 1:1.5 ratio, and then subjected to extraction with petroleum ether, dichloromethane, ethyl acetate, and methanol, each extracted twice. The collected fractions were concentrated under reduced pressure to obtain four crude extracts, designated as DSL-4-1 to DSL-4-4. DSL-4-3 (37.2 g) underwent silica gel chromatography (75~150 μm) and was eluted with dichloromethane-methanol gradients (20:1, 10:1, 5:1, 3:1), resulting in the isolation of four components

named DSL-4-3-1 to DSL-4-3-4. DSL-4-3-1 (13.97 g) underwent further purification by medium-pressure chromatography (10%~90% methanol, monitored at 210 nm, collected every 500 mL), resulting in the isolation of 40 components named DSL-4-3-1-1 to DSL-4-3-1-40. Preparative HPLC was utilized for further purification of the above components. The chromatographic conditions were as follows: DSL-4-3-1-17 (C18, 23% acetonitrile, flow rate: 3.0 $mL \cdot min^{-1}$, monitored at 210 nm), yielding compound **5** (19.8 mg); DSL-4-3-1-23 (C18, 15% acetonitrile-0.05% formic acid, flow rate: 3.0 $mL \cdot min^{-1}$, monitored at 210 nm), yielding compounds **6** (27.9 mg) and **7** (40.2 mg).

3.2. Antifungal Activity Assay of Monomeric Compounds

The mycelial growth rate method [22] was employed to assess the antifungal activity of the seven compounds dissolved in 50% methanol, with a final concentration of 100 $\mu g \cdot mL^{-1}$, against *P. herbarum*. The inhibitory activity was determined at this concentration. Futhermore, PDA culture media containing the compounds at concentrations of 25, 50, 100, 200, and 400 $\mu g \cdot mL^{-1}$ were prepared, and their antimicrobial activities were evaluated after inoculation and cultivation. The toxicity regression equation, effective concentration (EC_{50}) value, and coefficient of determination (R^2) were calculated. Eugenol was used as the positive control drug, with three replicates for each treatment group. The mycelial growth inhibition rate was calculated using the following formula:

$$\text{Antifungal rate } (\%) = \frac{(\text{diameter of control colony} - \text{diameter of treatment colony})}{(\text{diameter of control colony} - 0.5)} \times 100\%$$

3.3. Morphological and Ultrastructural Observation of P. herbarum

Optical Microscopy Observation: Fresh *P. herbarum* mycelial colonies were placed on PDA culture media containing 100 $\mu g \cdot mL^{-1}$ of the test compound. Blank controls were set up. After 5 days of incubation at a temperature of 28 ℃, humidity of 70%, and dark conditions, mycelia from the edges of the culture dishes were picked and placed on glass slides for observation of the differences in mycelial morphology between the control and treatment groups under an optical microscope.

Scanning Electron Microscopy Observation: After being suitably rinsed with PBS, an appropriate amount of mycelium was fixed for 2 hours at room temperature in 2.5% glutaraldehyde, and then it was thoroughly cleaned three times for 15 minutes each using 0.1 M phosphate buffer (pH 7.4). It was then fixed for 1 to 2 hours at room temperature in 1% osmium tetroxide in 0.1 M phosphate buffer. This was followed by three 15-minute washes in 0.1 M phosphate buffer. A succession of ethanol solutions (30%, 50%, 70%, 80%, 90%, 95%, and 100%) were used to dehydrate the material for 15 minutes each. This was followed by a 15-minute substitution period using isoamyl acetate. Using a K850 critical point drier, the samples were dried and sputter-coated with beneath an SU8100 scanning electron microscope after being coated in gold using an MC1000 ion sputter coater. [23].

Transmission Electron Microscopy Observation: Three times, an appropriate volume of fungal hyphae samples was fixed in 2.5% glutaraldehyde for 4 to 6 hours at room temperature. The samples were then rinsed with 0.1 M phosphate buffer (pH 7.4) for 15 minutes. After fixing the hyphae for 2 hours at room temperature with 1% osmium tetroxide in 0.1 M PBS buffer, the hyphae were washed three times for fifteen minutes each time using 0.1 M PBS buffer. The samples were then dehydrated in two stages using 100% ethanol and a gradient series of ethanol solutions (30%, 50%, 70%, 80%, 90%, and 100% v/v) for a total of 20 minutes per step. The dehydrated hyphae samples were sequentially treated with a permeating agent (acetone: epoxy resin - 2:1, acetone: epoxy resin - 1:1, epoxy resin) at 37°C for 10 hours. Following infiltration, the samples were embedded in embedding plates using epoxy resin. Polymerization was conducted at 60 °C for 48 hours, followed by 20 days at room temperature. Ultrathin sections (50 nm) were prepared using an ultramicrotome and stained with uranium-lead (2% uranyl acetate saturated aqueous solution, lead citrate) at room temperature for 15 minutes. The sections were air-dried overnight at room temperature before observation under a transmission electron microscope (TEM). [24].

3.4. Transcriptome Sequencing Analysis

The fungal mycelia of *P. herbarum* were cultured in PDB medium at 28 °C with shaking at 110 r/min for 3 days. For the treatment group, militarine was added to achieve a final concentration of 100 μg·mL^{-1}. Blank controls were set up under the same conditions. After 48 hours of cultivation, mycelia were harvested by centrifugation to obtain 0.5 g of fungal mycelia. The mycelia were washed three times with PBS buffer (pH= 7.2), then rapidly frozen in liquid nitrogen and sent to Suzhou Panomics Biotech Ltd. for transcriptome analysis. RNA extraction, library construction, library quality control, data quality control, RNA sequencing comparative analysis, gene analysis, sample relationship analysis, and inter-group differential analysis were conducted.

3.5. Effect of Militarine on Dry Weight of P. herbarum Mycelium

Militarine was prepared in PDB medium to achieve final concentrations of 25, 50, 100, 200, and 400 μg/mL. Five fungal cakes of *P. herbarum* were inoculated into each medium. Distilled water without the addition of the drug was used as a blank control, with three replicates for each treatment. The media were placed in an oscillating culture box (110 r/min, 28°C). After 6 days of cultivation, the mycelia in the media were collected, dried, and weighed.

3.6. Effect of Militarine on the Relative Conductivity of P. herbarum Cell Membranes

Five fungal cakes of 6-day-old *P. herbarum* were taken with a 5mm punch and inserted into the drug-containing PD medium, incubated with shaking for 6 days, collected, washed, and dried the mycelium with a final concentration of 100 μg/mL. 1 g of mycelium was taken in 25 mL of the solution, and the conductivity was measured after treatment for 0.5, 1.0, 1.5, 2.0, and 2.5 h, and the mycelium was boiled and cooled after treatment for 2.5 h to determine the final conductivity [25]. Using distilled water as a blank control, set up 3 replicates. The formula for calculating the relative conductivity of mycelium is given below:

$$\text{Relative conductivity (\%)} = \frac{\text{(conductivity at a certain time)}}{\text{(conductivity after fungal boiling to death)}} \times 100\%$$

3.7. Effect of Militarine on the Physiological and Biochemical Indicators of P. herbarum

Five well-growing fungal cakes of *P. herbarum* were inoculated into PDB medium and oscillated for 5 days. The militarine was dissolved in 50% methanol solution to attain a concentration of μg·mL^{-1} for the intended treatment. Sterile water without the drug was used as a blank control. Mycelia were collected at 1, 6, 12, 18, and 24 hours after treatment, with 0.4g collected each time and stored at -20°C for subsequent analysis. Changes in catalase (CAT), peroxidase (POD), superoxide dismutase (SOD), malondialdehyde (MDA), and reducing sugar content in *P. herbarum* treated with militarine were determined according to the methods provided by the assay kit (Solarbio Biochemical Kit) [21, 22, 25].

3.8. CLSM Observation of Militarine on the Hyphal cells of P. herbarum

3.8.1 Effect of Militarine on Reactive Oxygen Species (ROS) in Fungal Hyphae

Following the method described by Liu et al. [26], the level of ROS in *P. herbarum* was detected by DCFH-DA staining. Militarine was prepared in PDB medium to final concentrations of 0, 100, and 200 μg·mL-1. Well-growing strains were selected, and five fungal cakes were inoculated into each medium and oscillated for 3 days (110 r/min, 28°C). After washing with 0.01% PBS buffer, mycelia were incubated in 10 μmol/L DCFH-DA solution at 30°C in the dark for 30 minutes and observed under confocal laser scanning microscopy (CLSM). Parameter settings, using 488 nm excitation wavelength, 525 nm emission wavelength.

3.8.2 Effect of Militarine on the Integrity of Fungal Hyphal Cell Walls

Mycelia were prepared following the method described in section "3.8.1", referencing the method by Wang et al. [27], mycelia washed with 0.01% PBS buffer were placed on cover slips, stained with 20 μL of CFW for 1 minute, and observed under CLSM.

3.8.3 Effect of the Damage to Fungal Hyphal DNA by Militarine

Mycelia were prepared following the method described in section "3.8.1", referencing the method by Wang et al. [28], mycelia washed with 0.01% PBS buffer were suspended in 70% anhydrous ethanol and incubated at 4°C for 30 minutes. Subsequently, the mycelia were incubated in 5 $\mu g \cdot mL^{-1}$ DAPI solution in the dark for 30 minutes, and the fluorescence intensity was observed under CLSM.

4. Results and Discussion

4.1. Structural Identification

The structures of compounds **1-7** were identified using techniques such as ^{1}H-NMR, ^{13}C-NMR, and corroborated with previously reported spectral data to confirm their structures, as depicted in Figure 1.

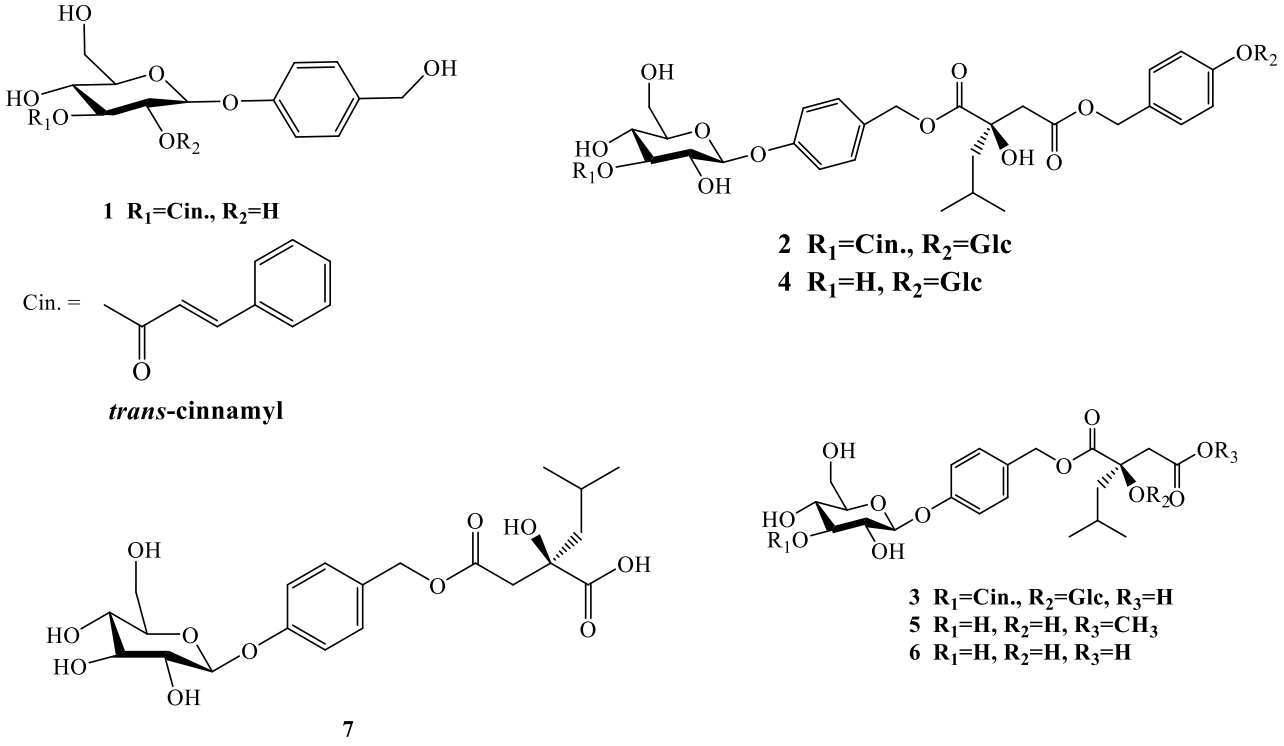

Figure 1. The structures of compounds **1-7**

*Compound **1***: $C_{22}H_{24}O_8$, pale yellow powder, ESI-MS *m/z*: 439 $[M+Na]^+$. The ^{1}H and ^{13}C NMR data are detailed in the supplementary information, which are almost identical to the literature values [28]. Therefore, this compound was identified as 1-*O*-(4-hydroxymethylphenoxy)-3-*O*-*trans*-cinnamoyl-*β*-D-glucoside.

*Compound **2***: $C_{43}H_{52}O_{18}$, yellowish oil, ESI-MS *m/z*: 857 $[M+H]^+$. The ^{1}H and ^{13}C NMR data are detailed in the supplementary information, which are almost identical to the literature values [29]. Therefore, this compound was identified as Pleioneside C.

*Compound **3***: $C_{36}H_{46}O_{17}$, yellowish oil, ESI-MS *m/z*: 751 $[M+H]^+$. The ^1H and ^{13}C NMR data are detailed in the supplementary information, which are almost identical to the literature values [29]. Therefore, this compound was identified as Pleioneside B.

*Compound **4***: $C_{34}H_{46}O_{17}$, white amorphous powder, ESI-MS m/z: 725 $[M-H]^-$. The ^1H and ^{13}C NMR data are detailed in the supplementary information, which are almost identical to the literature values [20]. Therefore, this compound was identified as militarine.

*Compound **5***: $C_{22}H_{32}O_{11}$, white gel-like substance, ESI-MS *m/z*: 471 $[M-H]^-$. The ^1H and ^{13}C NMR data are detailed in the supplementary information, which are almost identical to the literature values [30]. Therefore, this compound was identified as 1-(4-*β*-D-glucopyranosyloxybenzyl) 4-methyl (2R)-2-isobutylmalate.

*Compound **6***: $C_{21}H_{30}O_{11}$, white powder, ESI-MS *m/z*: 459 $[M+H]^+$. The ^1H and ^{13}C NMR data are detailed in the supplementary information, which are almost identical to the literature values [31]. Therefore, this compound was identified as gymnoside I.

*Compound **7***: $C_{21}H_{30}O_{11}$, white powder, ESI-MS *m/z*: 459 $[M+H]^+$. The ^1H and ^{13}C NMR data are detailed in the supplementary information, which are almost identical to the literature values [31]. Therefore, this compound was identified as gymnoside II.

4.2. Cytotoxic Activity Evaluation of Compounds

Table 1. Cytotoxicity equations of compounds against *P. herbarum*

compounds	Virulence regression equation (y=)	EC_{50}(μg/mL)	correlation coefficient (R^2)	95% confidence (μg/mL)
2	y = 1.341 x – 5.961	85.173	0.941	55.085-132.548
4	y = 0.660 x – 2.791	68.575	0.983	55.953-82.233
Eugenol	y = 1.049 x – 4.531	75.312	0.958	61.93-89.685

At a concentration of 100 μg/mL, compounds **2** and **4** demonstrated significant inhibitory effects against *Phoma herbarum*. Consequently, further cytotoxicity assays were performed on these two compounds. The results are tabulated in Table 1. Compound **4** revealed an EC_{50} of 68.575 μg/mL, and its cytotoxicity was more pronounced than that of the positive control, Eugenol. Consequently, its antifungal mechanism warranted comprehensive investigation.

4.3. Effects of Militarine on the Morphology

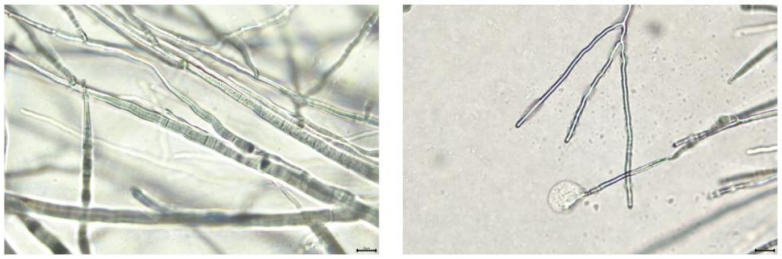

Figure 2. The effects of militarine on the morphology of *P. herbarum* hyphae

It (Figure 2) shows that, under optical microscopy, the hyphal morphology in the control group exhibited a normal, smooth surface, consistent thickness, and regular branching length, devoid of any visible fractures or disruptions. However, the hyphae in the treatment group seemed to be less robust and less plump, showing clear signs of intracellular content leakage. This observation indicates that Militarine treatment could potentially induce internal structural damage within the hyphae, potentially leading to the leakage of intracellular contents.

4.4. Effects of Militarine on the Ultrastructure of P. herbarum

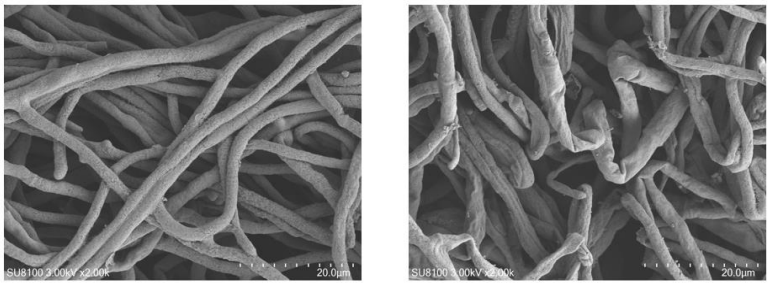

CK (20μm) 100 μg/mL(20μm)

Figure 3. Morphological structure of hyphae after treatment with militarine under scanning electron microscopy

Scanning electron microscopy analysis of fungal treated with militarine (Figure 3) demonstrated notable morphological changes in comparison to the untreated control group. On control group, the fungal hyphae typically presented with a rounded, plump morphology, characterized by uniform thickness, a smooth texture, and a cylindrical form. Such features denoted healthy growth. However, after it treated in militarine, these hyphae displayed structural instability, with a reduction in cohesion between filaments. This led to a withered and creased appearance, irregular thickness, local indentations, and, in extreme cases, hyphal breakage.

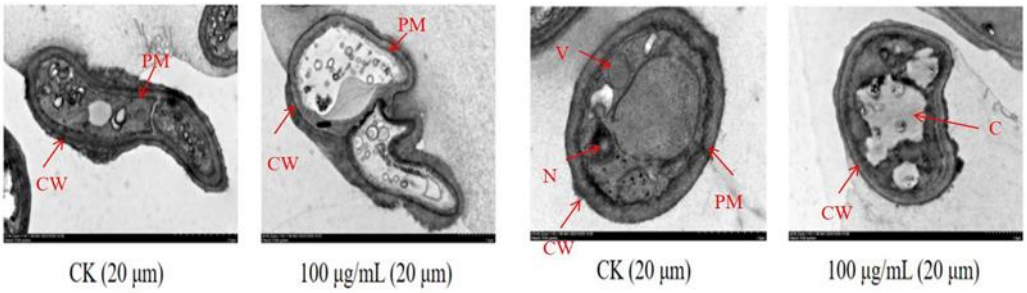

CK (20 μm) 100 μg/mL (20 μm) CK (20 μm) 100 μg/mL (20 μm)

Figure 4. Observation of fungal hyphae morphology under transmission electron microscopy (longitudinal sections on the left, cross Sections on the right)
N: nucleus; **PM**: plasma membrane; **CW**: cell wall; **V**: vesicle; **C**: cavity

As depicted in Figure 4, observation of hyphal cells under transmission electron microscopy revealed distinct morphological changes. In the control group, hyphal cells exhibited regular shapes, intact structures, uniform cytoplasm, well-defined cell walls, and clear plasma membrane edges, with homogeneous and dense cytoplasm. However, subsequent to treatment with 100 μg/mL of militarine, hyphal cells exhibit deformation, with damage to the cellular structure. Notably, the cell wall undergoes thinning, and the delineation between the cell wall and the plasma membrane becomes indistinct. Furthermore, the intracellular materials are compromised, leading to the formation of numerous cavities within the cells.

The fluorescence probe DCFH-DA is utilized to measure intracellular ROS levels. In the presence of reactive oxygen species (ROS), DCFH undergoes oxidation, generating 2',7'-dichlorofluorescein (DCF) and emitting green fluorescence, higher fluorescence indicates greater ROS accumulation [32]. As it can be seen (Figure 5A) that the intensity decay of fluorescence is proportional to the magnitude of the militarine concentration. With the concomitant escalation of treatment concentration, a conspicuous augmentation in fluorescence was discerned within the cellular milieu. Concurrently, a substantial elevation in the ROS content was observed within the mycelial framework. Such alterations suggest that militarine exerts its influence on the intracellular redox homeostasis, leading to a disruption of the redox equilibrium. Consequently, this imbalance impedes the normal functioning of the redox system, thereby curtailing the hyphal growth.

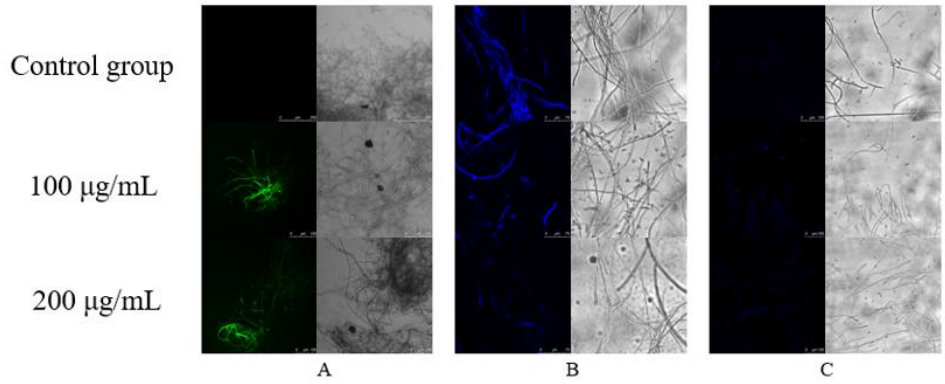

Figure 5. CLSM observation of militarine on the hyphal cells of *P. herbarum*

(**A)** The effect of militarine on ROS in fungal hyphae; the left side shows the ROS staining fluorescence image, and the right side shows the ROS staining bright-field image. (**B**) The effect of militarine on the integrity of fungal hyphal cell walls; the left side shows the CFW staining fluorescence image, and the right side shows the CFW staining bright-field image. (**C**) The effect of the damage to fungal hyphal DNA by militarine; the left side shows the DAPI staining fluorescence image, and the right side shows the DAPI staining bright-field image.

CFW, a non-specific fluorescent brightening dye, attaches to cellulose and chitin, indicating alterations in cell wall structure. As depicted in Figure 6, following 24 hours of militarine treatment at various concentrations (100 and 200 μg/mL), the blue fluorescence intensity of *P. herbarum* hyphae decreased progressively compared to the control group. As observed (Figure 5B) that the modulation of blue fluorescence intensity associated with hyphal architecture in response to increasing concentrations of militarine. The observed attenuation in fluorescence intensity correlates inversely with the magnitude of militarine concentration, suggesting a progressive depletion of cellulose and chitin, principal constituents of the fungal cell wall. This alteration in cell wall composition is indicative of structural reorganization. This indicates that militarine exerts its inhibitory effects on the growth of *P. herbarum* by disrupting the normal integumentation of the fungal cell wall. This interference results in cellular stress, compromising the integrity and functionality of the cell wall, and ultimately thwarts the fungal colonization process.

DAPI (4', 6-diamidino-2-phenylindole) fluorescent dye was used to detect the damage of militarine to the nucleus of *P. herbarum*. DAPI can bind to DNA to form complexes that emit high-intensity light blue fluorescence [33]. The results (Figure 5C) demonstrated that the hyphae in the control group exhibit punctate blue fluorescence under microscopic examination, suggesting that the DNA structure within the hyphae is stable, and the nuclei are clearly distinguishable. However, after treating the hyphae with concentrations of 100 and 200 μg/mL militarine for a 24-hour period, a gradual reduction in the intensity of blue fluorescence was observed. Concurrently, the fluorescence transitioned from a punctate to a streak pattern, indicating alterations in the DNA within the nuclei. This observation suggests that the hyphae experienced nuclear DNA damage in response to militarine exposure, which may account for the attenuation of fluorescence intensity and the subsequent change in fluorescence distribution pattern.

4.5. Study on the Antifungal Mechanism Based on Transcriptomics

4.5.1 Assessment of Raw Sequencing Data Quality

Table 2. Summary of quality control data

Sample	Reads No.	Bases(bp)	Q30(bp)	N(%)	Q20(%)	Q30(%)
Ck-1	36554846	5519781746	5267687196	0.002419	97.49	95.43
Ck-2	42813018	6464765718	6178313686	0.002341	97.56	95.57
Ck-3	37914346	5725066246	5466464311	0.002418	97.51	95.48
S-1	36174224	5462307824	5212309158	0.002377	97.48	95.42
S-2	37591780	5676358780	5411577053	0.002392	97.45	95.34
S-3	43600874	6583731974	6287517192	0.002409	97.52	95.50

RNA sequencing was conducted on *P. herbarum* treated with militarine as the experimental group. As shown in Table 2, among the 6 samples, the Q20 values for the blank control ranged from 97.49% to 97.56%, with the lowest Q30 value not less than 95.43%. For the treatment group, the Q20 values ranged from 97.45% to 97.52%, with the lowest Q30 value not less than 95.34%. The balanced nucleotide composition indicates high sequencing quality, leading to more accurate subsequent analyses.

4.5.2 Analysis of Differential Gene Expression

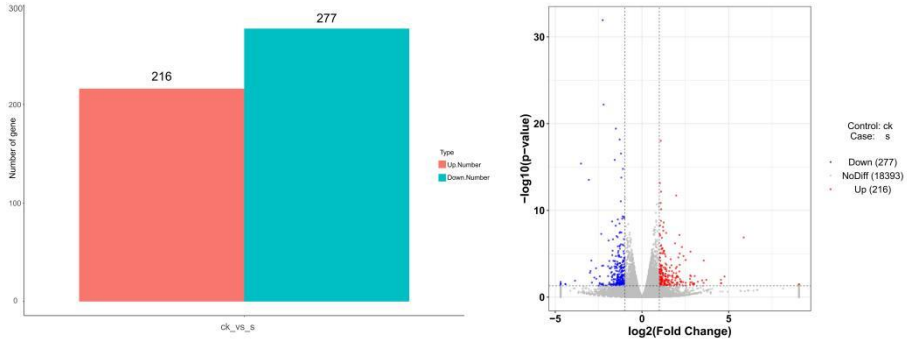

Figure 6. Statistical analysis of differential expression results (Left) and volcano plot of differentially expressed genes (Right)

Sequencing was performed on *P. herbarum* before and after treatment with militarine. DESeq software was used to analyze the differential gene expression between the two groups. The criteria for selecting differentially expressed genes were as follows: significant P-value < 0.05 and expression fold change |log2 Fold Change| > 1. The analysis revealed significant changes in gene expression in the *Phoma herbarum* after treatment. A total of 493 expressed genes showed significant changes, with 216 genes up-regulated and 277 genes down-regulated differentially (Figure 6).

4.5.3 GO Enrichment and KEGG Pathway Analysis of Differentially Expressed Genes

In comparison with the control group, 464 differentially expressed genes were annotated to GO functional terms. Among them, 205 genes were notably upregulated, while 259 genes were downregulated. Most of these genes were associated with biological processes (BP), with 271 showing significant differences. This subset comprised 102 upregulated and 169 downregulated genes. Specifically, 107 of the differentially expressed genes were linked to metabolic processes, and 48 were associated with biosynthetic processes. Specifically, genes involved in secondary metabolic processes were significantly upregulated, while those related to biosynthetic processes were significantly downregulated, suggesting that the increase in secondary metabolites may lead to the formation of abundant attachments within the mycelium, while the decrease in biosynthesis may result in slower mycelial growth [34]. The molecular function (MF) category included 169 differentially expressed genes, with 37 genes involved in binding and 36 genes involved in catalytic activity.

The cellular component (CC) category included 34 significantly different genes, with 26 differentially expressed genes belonging to membrane-related components. As shown in Figure 7, differentially expressed genes were mainly distributed in cellular metabolic processes, biosynthetic processes, catalytic reactions, organelles, and cell membrane components

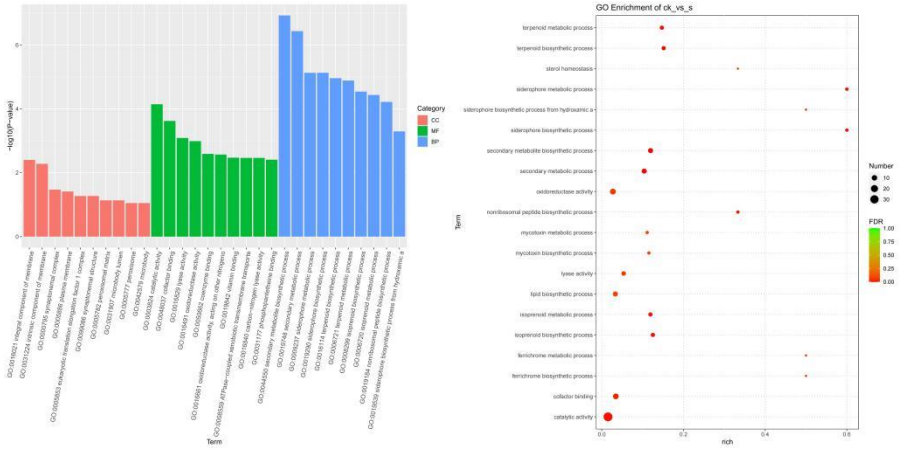

Figure 7. Gene ontology (GO) enrichment analysis bar chart and bubble chart

GO biological enrichment analysis of differentially expressed genes was conducted using the DAVID database with a screening criterion of $P < 0.05$. The results of GO enrichment analysis for differentially expressed genes were classified into molecular function (MF), biological process (BP), and cellular component (CC) categories. The top 10 significantly enriched GO terms with the smallest p-values were selected for each GO category for display.

.

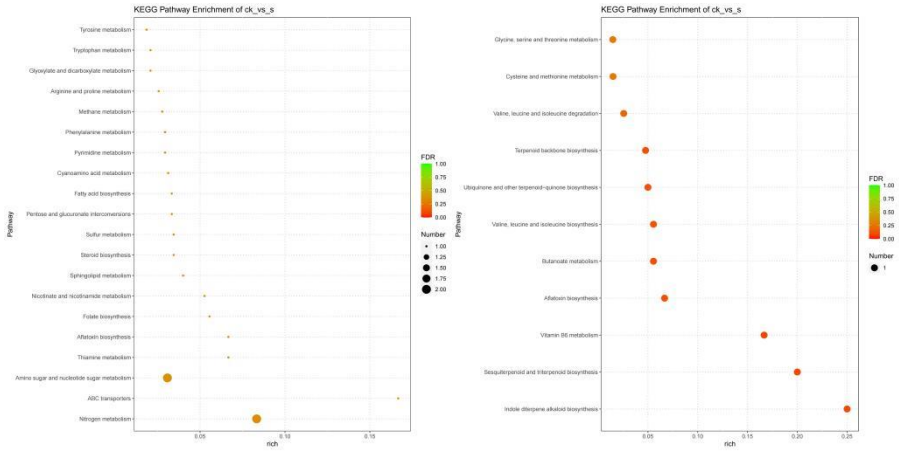

Figure 8. KEGG Pathway analysis (left: upregulated genes, right: downregulated genes)

The differentially expressed genes underwent KEGG pathway analysis, revealing 33 pathways with distinct gene expression between the treatment and control groups. These pathways included 30 metabolic pathways, along with one each for cellular processes, environmental information processing, and genetic information processing. As depicted in Figure 8, among the upregulated gene-associated pathways, 20 were notably enriched in metabolic pathways, particularly nitrogen metabolism, and environmental information processing, specifically ABC transporters. For pathways linked to downregulated genes, 11 showed significant enrichment, encompassing indole alkaloid biosynthesis, sesquiterpenoid and triterpenoid biosynthesis, and vitamin B6 metabolism. Nitrogen metabolism is a crucial physiological process that influences fungal metabolism and development [35]. Studies have

indicated that [36] increased nitrogen promotes fungal infection, while heightened nitrogen metabolism inhibits it. In this study, significant up-regulation of differential genes affecting nitrogen metabolism was observed in the treatment group. This suggests that the external interference induced by militarine may have triggered the fungus to enhance their resistance to the internal environmental changes brought about by militarine. By activating nitrogen metabolism, the fungus itself could potentially modulate their growth and hyphal infection potential. This finding highlights the complex interplay between external stressors and bacterial physiological responses, underscoring the importance of understanding the molecular mechanisms underlying microbial adaptation to environmental changes.

ABC transporters are prevalent transport proteins involved in molecular transmembrane transport [36]. They primarily utilize ATP to transport various substances like sugars, amino acids, and proteins across biological membranes. Some inward transport proteins aid in transporting amino acids, sugars, and other nutrients from the extracellular environment into the intracellular matrix, promoting cell growth [37]. This type of protein can be divided into two categories according to its transport direction: one is the inward transporter, which can transport nutrients such as amino acids and sugars from the external environment to the inside of the cell to promote cell growth; The other type is the outward transporters, which are responsible for the "detoxification" effect, which can excrete substances harmful to cell growth such as antibiotics and fatty acids from the cell, help the cell maintain exogenous substances or unnecessary secondary metabolites at low concentrations, reduce the burden of cell growth, maintain normal cell growth, and significantly improve the survival rate of cells [38]. Differential genes of the ABC transport system were significantly enriched after militarine treatment, suggesting that the addition of militarine stimulates cells to eliminate harmful substances from the environment by activating the ABC transport system to mitigate toxic effects and maintain cellular homeostasis.

5.5. Effect of Militarine on the Physiological and Biochemical Indicators of P. herbarum

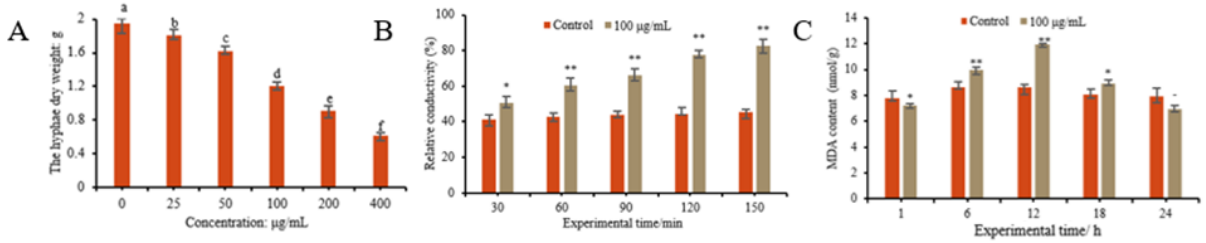

Figure 9. Effects of militarine on the hyphae dry weight, relative conductivity and MDA content of hyphae

It shows that (Figure 9A), after 6 days of militarine treatment, there was a notable suppression of mycelial growth in *P. herbarum*. With increasing militarine concentration, the mycelial dry weight significantly decreased compared to the control group. At a concentration of 400 μg·mL^{-1} in the treatment group, the mycelial dry weight was 0.6120 g, markedly lower than the control group's 1.9455 g.

When fungal hyphal cell membranes rupture, causing the leakage of intracellular substances, the conductivity of the extracellular solution increases [39]. Through assessing the relative conductivity of mycelial solution post-militarine treatment, we observed a significant increase compared to the control group. Additionally, as treatment duration increased, the relative conductivity of fungal cells rose, reaching 82.8% at 150 minutes (Figure 9B). This rise in permeability of the fungal cell membrane led to cytoplasm leakage. With prolonged treatment, damage to the fungal cell membrane intensified. This suggests that militarine disrupts cell membrane permeability, resulting in hyphal content leakage, elevated conductivity, and triggering osmotic stress response in fungi.

Under external environmental stress conditions, malondialdehyde (MDA) is one of the most important products of membrane lipid peroxidation. It can affect DNA, membrane proteins, and enzymes, increasing cell membrane permeability, thereby leading to changes in membrane structure, function, and metabolism. Therefore, MDA content can be used to reflect the extent of membrane damage [40].

Under the condition of a drug concentration of 100 μg/mL, the MDA content was close to that of the control group after 1 hour of treatment. However, the MDA content in the treatment group sharply increased with prolonged time, reaching a peak at 12 hours (11.935 nmol·g^{-1}), followed by a gradual decrease (Figure 9C). In contrast, the MDA content in the control group remained almost unchanged throughout the entire experiment and was consistently lower than that in the treatment group, indicating that militarine can induce MDA accumulation in hyphae, leading to lipid peroxidation of the cell membrane and oxidative damage.

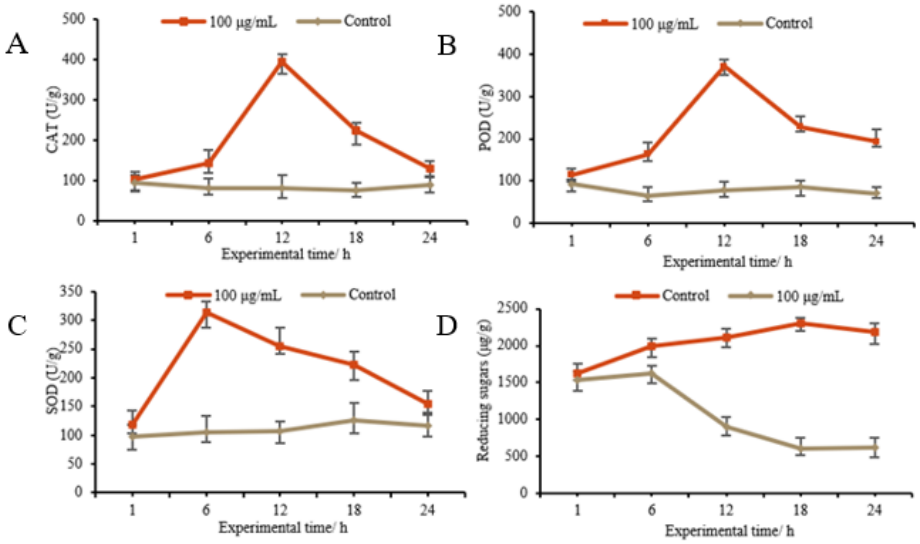

Figure 10. Effects of militarine on the activities of three protective enzymes and the content of reducing sugars in hyphae

During invasion, plant pathogens trigger physiological and biochemical defense responses, including changes in antioxidant and defense enzyme activities. Studies reveal that superoxide dismutase (SOD), peroxidase (POD), and catalase (CAT) are products of stress-induced defense mechanisms in plant pathogens [41-43]. In this study (Figure 10), militarine treatment effects on these enzyme activities in *P. herbarum* hyphae are demonstrated. At 100 μg·mL^{-1} concentration, enzyme activities initially increased and then declined with prolonged treatment. Conversely, enzyme activities in the control group remained relatively stable, CAT activity peaked at 12 hours (393.24 U/g), 4.83 times higher than the control (Figure 10A). POD activity trended similarly, peaking at 12 hours (370.916 U/g), 4.72 times higher than the control (Figure 10B). SOD activity reached its peak at 6 hours (312.94 U/g), 2.97 times higher than the control (Figure 10C). These findings suggest that militarine treatment enhances enzyme activities in *P. herbarum* hyphae to counter self-toxicity. However, as stress escalates, protective enzyme activities decrease, disrupting hyphal physiological metabolism and inhibiting growth.

Reducing sugars serve as the primary energy source for hyphal growth maintenance [44]. After treatment with 100 μg/mL of militarine, the content of reducing sugars in the hyphae of *Phoma herbarum* significantly decreased (Figure 10D). From 6 to 18 hours of treatment, there was a substantial reduction in the content of reducing sugars within the fungal hyphae. At 18 hours, the content of reducing sugars was only one-third of that in the control group, stabilizing thereafter until 24 hours. This indicates significant damage to the hyphal structure post-treatment, resulting in substantial leakage of intracellular reducing sugars. Consequently, the normal energy metabolism process crucial for hyphal growth of *P. herbarum* is disrupted, leading to inhibited growth.

5. Conclusion

In this study, chromatographic methods such as macroporous adsorption resin, silica gel column chromatography, preparative liquid chromatography, and semi-preparative liquid chromatography were utilized to isolate and purify antibacterial active components from *Pleione bulbocodioides* of pseudobulbs. Modern spectroscopic techniques were then employed to identify seven butanedioic acid compounds, with compounds **1-3**, **5**, and **6** being newly isolated from *Pleione bulbocodioides*. Seven compounds were tested for antifungal activity against *P. herbarum*, revealing compound **4** (militarine) as the most potent inhibitor at 100 μg/mL concentration, with an EC_{50} of 68.575 μg/mL, surpassing the positive control, eugenol. Consequently, further investigation into its antifungal mechanism was pursued.

Observations of *P. herbarum* under optical microscopy, scanning electron microscopy, and transmission electron microscopy revealed significant morphological changes in the treated group, including distortion and folding of hyphae, deformation of hyphal plasma membranes, organelle degradation, and the formation of numerous cavities, indicating a pronounced morphological effect of militarine on *P. herbarum*. The experimental results showed that with the increase of treatment concentration, the content of ROS in mycelium increased significantly, and the cellulose and chitin in the cell wall gradually decreased, resulting in the disorder of the intracellular redox system, the structural integrity of the cell wall was destroyed, and the DNA in the nucleus was damaged.

Transcriptomic analysis was conducted to analyze the differential gene expression in hyphae (control group and 100 μg/mL militarine-treated group), identified 493 significantly differentially expressed genes, including 216 upregulated genes and 277 downregulated genes. GO analysis of these differentially expressed genes revealed enrichment primarily in biological process GO terms related to metabolism, biosynthesis, and oxidation-reduction processes. Significantly differentially expressed genes in cellular components were mainly distributed in membrane components, while those in molecular function were primarily related to catalytic and transport activities. KEGG pathway analysis indicated enrichment in pathways such as nitrogen metabolism, ABC transporters, alkaloid biosynthesis, terpenoid biosynthesis, and vitamin B6 metabolism.

The effect of militarine on the physiological and biochemical indexes of *P. herbarum* was further determined. The results showed that militarine could significantly inhibit the normal growth of *Phoma herbarum* hyphae, and the dry weight of mycelium was significantly reduced. Through the determination of the enzyme activity system, the treatment time was 1-24 h, and the activities of the three protective enzymes increased first and then decreased, indicating that when militarine poisoned *P. herbarum*, the activities of the three protective enzymes increased in order to self-defend to reduce the degree of self-toxicity. With the extension of the treatment time, the stress degree deepened, the mycelium structure was seriously damaged, and the activity of the protective enzyme decreased, which reduced the detoxification ability of the bacteria itself. Consequently, the normal growth and metabolism process of the hyphae was destroyed, thereby inhibiting the normal growth of *P. herbarum*.

The experimental results also showed that the relative conductivity and malondialdehyde content of the hyphae of *P. herbarum* after treatment with militarine increased significantly. This indicates that the permeability of the mycelial cell membrane was changed, and militarine destroyed the structure of the hyphal cell membrane, causing the membrane lipid peroxidation reaction. This led to a large amount of reducing sugar leakage of cell contents, which seriously affected the energy metabolism process of mycelial growth. Ultimately, this inhibited the normal growth of *P. herbarum*. These findings provide valuable insights into the mechanism of action of militarine on *P. herbarum*, which may contribute to the development of novel strategies for controlling the growth of *P. herbarum*.

Acknowledgments

This work was supported by the Natural Science Foundation of Fujian Province (2022J01244), the Major project of postgraduate teaching and research in undergraduate colleges and universities in Fujian Province (FJBKJY20220170), the Distinguished Young Talent Program of Fujian Agriculture and Forestry University (Xjq202103), and the Funding for visiting and research of Haixia Institute of Science and Technology (KFXH23026).

Supporting Information

Supporting information accompanies this paper on http://www.acgpubs.org/journal/records-of- natural-products

ORCID

Shilin Liu: 0000-0003-4474-2631
Jiarui Fu: 0009-0000-4376-3065
Yuping Fu: 0000-0003-3647-4147
Yuanan Chen: 0000-0002-5684-9340
Lijun Zhen: 0000-0002-2383-6930
Huiyou Xu: 0000-0001-5752-2932
Lin Ni: 0000-0001-6118-6724

References

[1] D. Q. Zhou and S. J. Xu (2005). Microbiology Dictionary. Tianjin Science and Technology Press.
[2] L. Y. Yang, Y. Wang, Y. H. Cheng, R. F. Gao, Q. Xu, B. L. He and H. X. Liu (2016). Study on the biological characteristics of *phoma* spp., *J. Shandong Agric. Univ. (Nat. Sci.)*. **47**, 501-505.
[3] X. H. Xu, H. Curt and P.H. Williams (1987). Differentiation of pathogenic and non-pathogenic isoiates of P*homa lingam*, *Acta Phytopathol. Sin.* 11-15.
[4] G. Y. Li, Y. Z. Ren and Q. Y. Wang (2001). Identification of pathogen populations during sugar beet seedling stage in Xinjiang, *Sugar. Crops. China.* 25-29.
[5] W. Yang, Y. Chen, X. J. Chen, Y. J. Yao and Y. F. Zhou (2016). A new disease of tea plant caused by *Phoma adianticola*, *J. Tea Sci.* **36**, 59-67.
[6] F. F. Wang, T. Tang, G. B. Fang, B. Yuan, J. Guo, Y. Y. Duan, X. L. Xiao, and J. M. You (2021). Study on the biological characteristics, insecticide screening and field control effect of leaf spot Bacteria *phoma herbarum* in atractylodes macrocephala, *J. Chin. Med. Mater.* **44**,1810-1814.
[7] W. J. Lu, S. G. Lou, C. H. Li, Y. Q. Yan, C. X. He, D. W. Sun, G. F. Yin and L. H. Wang (2016). Study on the biological characteristics of the pathogenic bacteria of buckwheat ring disease, *J. Anhui Agric. Univ.* **43**, 799-803.
[8] Z. M. Gu, Y. Z. Zou, D. D. Liang and M. S. Ji (2020). Formula selection of *Phoma herbarum* SYAU-06 water dispersible granule against dayflower, *Chin. J. Pestic. Sci.* **22**, 877-883.
[9] J. Zou, C. W. Yao, B. X. Deng, S. H. Li and Z. Zhou (2018). Pathogen isolation and identification of leaf spot disease of *polygonatum sibiricum*, *J. Huaihua Univ.* **37**,1-4.
[10] J. Q. Zhu, M, Wei, W. Zhang, Y, Liu, B. Z. Fu and G. Y. Li (2018). Biological characteristics of *Alternaria alternata* in white waterlily and screening of its indoor control agents, *Jiangsu. Agr. Sci.* **46**, 109-111.
[11] C. C. Zhang, W. H. Wu, Y. Q. Liang, J. L. Zheng, J. G. Xi, X. L. Zheng, W. Tang, P. D. Xu, R. li, C. P. He and et.al (2016). Pathogen identification and biological characteristics of leaf spot disease of kinggrass, *Jiangsu. Agric. Sci.* **44**, 210-214.
[12] X. Z. Zhao, Z. Chen, L. Yu, D. Y. Hu and B. A. Song (2018). Investigating the antifungal activity and mechanism of a microbial pesticide Shenqinmycin against *Phoma sp.*, *Pestic. Biochem. Physiol.* **147**, 46-50.
[13] X. X. Liu, H. D. Liu, L. L. Pan, Y. F. Wu, N. Wan, X. Zhou and B. Li (2019). Research progress on chemical constituents and bioactivities of plants of *Pleione bulbocodioides* (Franch.) Rolfe, *J. Jiangxi Univ. Chinese. Med.* **31**, 106-111.
[14] S. S. Wu, W. Li, L. M. Shen, C. R. Li, and X. Y. Lin (2019). *Pleione bulbocodioides* (Franch.) Rolfe: misty realm "fairy flower", *Forest Humankind.* 68-77.
[15] Edited by the Chinese Pharmacopoeia Commission (2015). Chinese Pharmacopoeia (2015 edition). Beijing: China Medical Science and Technology Press.

[16] H. L. Dong, S. X. Guo, C. L. Wang, J. S. Yang and P. G. Xiao (2007). Advances in studies on chemical constituents in plants of *Pseudobulbus Cremastrae seu Pleiones* and their pharmacological activities, *Chin. Tradit. Herb. Drug*. 1734-1738.

[17] C. Wang, S. S. Hang, B. S. Cui, X. J. Wang and S. Li (2014). Chemical constituents from *Pleione bulbocodioides*, *China J. Chin. Mater. Med.* **39**, 442-447.

[18] X. Q. Liu, D. R. Wan and Q. Y. Yuan (2011). The chemical composition of the Chinese herb *Pleione bulbocodioides*, *Chin. J. Hosp. Pharm.* **31**, 1649-1650.

[19] F. Zhang, M. B. Zhao, J. Li and P. F. Tu (2013). Chemical constituents from *Pleione bulbocodioides*, *Chin. Tradit. Herb. Drug*. **44**, 1529-1533.

[20] S. W. Han, C. Wang, B. S. Cui and S. Li (2015). Studies on glucosyloxybenzyl 2-isobutylmalates of *Pleione bulbocodioides*, *China J. Chin. Mater. Med.* **40**, 908-914.

[21] J. R. Fu, S. L. Liu, Z. Y. Niu, L. J. Zheng, H. Y. Xu and L. Ni (2024). Antifungal activity of *Pleione bulbocodioides* (Franch.) Rolfe extract against plant pathogenic fungi, *J. Biosaf.* **33**, 77-82.

[22] Z. Z. Pan, J. R. Fu, W. Zheng, S. L. Geng, L. J. Zhang, H. Y. Xu and L. Ni (2022). Inhibitory activity ofIsoflavones from Ormosia hosiei Seeds against Botrytis cinerea, *J. Fujian Agric. Sci*. **37**, 794-801.

[23] H. W. Zhang, R. T. Chen, J. J. Xu, J. H. Zhou, P. Shi, Q. S. Yang, J. Han, K. Chu, J. Yu and D. F. Chi (2024). Scanning electron microscopy and pathogenicity of *Beauveria bassiana* infection with *Hylurgus ligniperda*, *J. Cent. South Univ. For. Technol.* **44**, 62-72.

[24] P. S. Shankar, J. Xu, A. D. S, J. Y. Li and N. Wang (2023). Microscopic and transcriptomic analyses of early events triggered by *'Candidatus Liberibacter* asiaticus' in young flushes of huanglongbing-positive citrus Trees, *Phytopathology*, **113**, PHYTO10220360R-PHYTO10220360.

[25] Y. Zhang, Z. Y. Lin, W. J. Zhou, Z. Z. Pan, J. R. Fu, J. X. Chen, L. Ni and S. Q. Zou (2021). Chemical constituents against *Phvtophthora capsici* from twigs of *Euscaphis konishii Hayata*, *J. Fujian Agric. For. Univ.* **50**, 472-479.

[26] H. L. Liu, J. K. Wang, J. B. Deng, L. Hu, S. M. Liu, L. Zhang and B. Liu (2015). Protection of danshen formula granula against damage of pc12 cells induced by alcohol, *Chin. Tradit. Herb. Drugs*. **46**, 1800-1805.

[27] F. T. Wang, P. P. Ji, F. Liu, Z. L. Sun, H. H. Wu, D. Y. Wang, X. X. Xu, and, W. M. Xu (2018). Antimicrobial activity and mechanism of lactic acid on *Enterococcus faecalis*, *Jiangsu J. Agric Sci*. 34, 200-206.

[28] J. Wang, W. Zhang, L. Fan, A. W. Xie, H. J. Yang, S. Wei, H. C. Qu, Y. S. Hu and Y. Y. Lyu (2023). Inhibition mechanism of a soil-derived *Bacillus velezensis* strain on *Aspergillus flavus* growth, *J. Henan Univ. Technol., Nat. Sci. Ed.* **44**, 68-74.

[29] Z. W. Wang, Y. Li, D. H. Liu, Y. Mu, H. J. Dong, H. L. Zhou, L. P. Guo and X. Wang (2018). Four new phenolic constituents from the rhizomes of *Gastrodia elata Blume*, *Nat. Prod. Res.* **33**, 1140-1146.

[30] M. T. Wu, X. Q. Wu, L. J. Zheng, L. J. Zhang, J. R. Fu, X. Q. Zhang, S. S. Wu, and L. Ni (2021). Discovery of glucosyloxybenzyl 2-hydroxy-2-isobutylsuccinates with anti-inflammatory activities from *Pleione grandiflora*, *Fitoterapia* **155**, 105062.

[31] Y. Wang, S. H. Guan, Y. H. Meng, Y. B. Zhang, C. R. Cheng, Y. Y. Shi, R. H. Feng, F. Zeng, Z. Y. Wu, J. X. Zhang et al (2013). Phenanthrenes, 9,10-dihydrophenanthrenes, bibenzyls with their derivatives, and malate or tartrate benzyl ester glucosides from tubers of *Cremastra appendiculata*, *Phytochemistry* **94**, 268-276.

[32] T. Morikawa, H. H. Xie, H. Matsuda and M. Yoshikawa (2006). Glucosyloxybenzyl 2-Isobutylmalates from the tubers of *Gymnadenia conopsea*, *J. Nat. Prod.* **69**, 881-886.

[33] Patcharawalai W, Suchittra P and Chanchai B (2018). Oxidative stress in urothelial carcinogenesis: Measurements of protein carbonylation and intracellular production of reactive oxygen species, *Methods Molecular Biol. (Clifton, N.J.)*. **1655**, 109-117.

[34] Y. L. Xin, J. Wang, H. J. Yang, A. Lyu, W. Zhang, S. Wei, Y. S. Hu and Y. Y. Lyu (2022). Inhibitory effect and mechanism of antibacterial peptide Hst5 on *Fusarium moniliforme*, *J. Food Saf. Qual.* **13**, 7174-7182.

[35] H. J. Ma, C. Y. Hu, Y. K. Chen and H. Cao (2023). Effects of Clove and Licorice extracts on *Fusarium oxysporum* based on transcriptomics, *J. Shanxi. Agric. Sci.* **51**, 682-689.

[36] B. Yang, Y. Chen, X. Li, C. G. Ren and C. C. Dai (2013). Research progress on endophyte-promoted nitrogen assimilation and metabolism, *Acta Ecol. Sin.* **33**, 2656-2664.

[37] X. Z. Wang, W. M. Sun, Y. F. Ma, E. Q. Han, L. Han, L. P. Sun, Z. H. Peng and B. J. Wang (2017). Research progress of ABC transporters in *Arabidopsis thaliana*, *Plant Physiol. J.* **53**, 133-144.

[38] D. B. Chen, J. Y. Wang, C. W. Xiao, Y. L. Wang and G. C. Sun (2021). Research progress in structure of ABC transporters and their function in pathogenic fungi, *Prog. Biochem. Biophys.* **48**, 309-316.

[39] J. Z. Qu, T. H. Chen, M. D. Yao, Y. Wang, W. H. Xiao and B. Z. Li (2020). ABC transporter and its application in synthetic biology, *Chin. J. Biotechnol. (1985-)* **36**, 1754-1766.

[40] X. Q. Chen, Y. Y. Zhao, Z. Zhang, P. J. Wu, W. Li, J. M. Du, S. X. Zhang, P. Wang and L. Wang (2022), Analysis of cinnamon essential oil composition and its mechanism of cell membrane damage in Salmonella enterica, *Food Ferment. Ind.* **48**, 24-32.
[41] D. C. Yin, X. Deng, I. Chet and R. Q. Song (2014). Inhibiting effect and mechanism of Trichoderma virens T43 on four major species of forest pathogen, *Chin. J. Ecol.* **33**,1911-1919.
[42] Z. M. Wu, M. Zhong, C. J. Lu, P. Liu, Z. H. Zhan, K. S. Shao and K. T. Li (2018). Effects of the crude extract from *Streptomyces sp.* N2 on cell membrane and antioxidant function of *Rhizoctonia solani*, *J. Nucl. Agric. Sci*. **32**,700-707.
[43] L. H. Wu, Y. F. Chen, P. Chen and H. L. Yi (2016). Sodium arsenite exposure affects the levels of antioxidant enzymes and lipid peroxidation in *Saccharomyces cerevisiae*, *Asian J. Ecotoxicol.* **11**, 302-307.
[44] J. J. Wang, X. F. Shao, S. M. Liu, F. Xu and H. F. Wang (2016). Effect of tea tree oil on the physiological function of *Botrytis cinerea*, *Mod. Food Sci. Technol*. **32**,56-62.
[45] T. Yang, Q. Q. Li, H. A. Shi, M. F. Wu, Z. L. Zhang, and L. H. Wang (2018). Antifungal mechanism of 3 kinds of phenols against *Colletotrichum gloeosprioides*, *Jiangsu. Agric. Sci.* **46**,106-109.